Quantum Disordering of an Antiferromagnetic Order by Quenched Randomness in an Organic Mott Insulator

Mizuki Urai,[1] Kazuya Miyagawa,[1] Takahiko Sasaki,[2] Hiromi Taniguchi,[3] and Kazushi Kanoda[1]
[1]Department of Applied Physics, University of Tokyo, Tokyo 113-8656, Japan
[2]Institute for Materials Research, Tohoku University, Sendai 980-8577, Japan
[3]Department of Physics, Saitama University, Saitama 338-8570, Japan

(Received 4 August 2019; accepted 18 February 2020; published 19 March 2020)

The behavior of interacting spins subject to randomness is a longstanding issue and the emergence of exotic quantum states is among intriguing theoretical predictions. We show how a quantum-disordered phase emerges from a classical antiferromagnet by controlled randomness. ^{1}H NMR of a successively x-ray-irradiated organic Mott insulator finds that the magnetic order collapses into a spin-glass-like state, immediately after a slight amount of disorder centers are created, and evolves to a gapless quantum-disordered state without spin freezing, spin gap, or critical slowing down, as reported by T. Furukawa *et al.* [Phys. Rev. Lett. **115**, 077001 (2015)] through sequential reductions in the spin freezing temperature and moment.

DOI: 10.1103/PhysRevLett.124.117204

The search for quantum spin liquids (QSLs) [1–4], in which spins are interacting without symmetry-breaking order at absolute zero, is a long-standing issue in solid-state physics. A key to realizing QSLs is the frustration in antiferromagnetic (AF) interactions. At present, there exist experimentally promising QSL candidates among geometrically frustrated triangle-based lattices, such as triangular [5–12], kagome [13–16], and hyperkagome [17,18] lattices. On the other hand, it has been theoretically suggested that randomness can also induce QSL states [19–21]. Indeed, several experimental works report on disorder-driven QSLs; for example, in a pyrochlore-type spin ice material, quenched structural disorder is argued to act as a transverse field on the non-Kramers f ions and induce a robust QSL state [22] and, in an organic Mott insulator with a quasitriangular lattice, an AF order gives way to a gapless QSL when randomness is introduced by x-ray irradiation [23]. Then, a question arises: how does the AF order evolve into the suggested QSL with increasing quenched disorder? The present work has tackled this issue, using the organic system under the systematic control of quenched disorder.

The layered organic compound, κ-$(ET)_2Cu[N(CN)_2]Cl$ (abbreviated as κ-Cl hereafter), where ET is bis(ethylenedithio)tetrathiafulvalene, is an ambient-pressure Mott insulator with an anisotropic triangular lattice with the anisotropy of transfer integrals, $t'/t = 0.4$–0.5 [24,25] (see the Supplemental Material [26] for the crystal structure). Below 23 K at zero magnetic field, κ-Cl exhibits a long-range AF order [30] carrying the moment of $0.45\mu_B$ per ET dimer at low temperatures, where μ_B is the Bohr magneton [31]. When pressure is applied, κ-Cl undergoes a first-order Mott transition to metal, which exhibits superconductivity below 13 K near the Mott critical pressure of 20–30 MPa [32].

Recent studies on κ-type ET compounds under x-ray irradiation has cast light on the impact of quenched disorder on the transport and magnetic properties of correlated electrons near the Mott transition [33]. By x-ray irradiation, the insulating behavior of κ-Cl is depressed with a resistivity drop by orders of magnitude and a decrease in the activation energy [33]. Furthermore, the AF spin order is suppressed [23,34] and gapless spin excitations emerge without indications of spin freezing, spin gap, or critical slowing down, suggesting a quantum-disordered spin state [23]. Infrared spectroscopy measurements [33,35] and first-principles calculations [36] suggest that the x-ray irradiation causes randomness in the chemical bonds in the anion layers, which disorders the periodic potential in the conducting ET layers.

Here, we reveal a detailed pathway from the AF ordered state to the QSL opened by randomness in successively x-ray-irradiated κ-Cl thorough probing the spin states by ^{1}H NMR measurements. The intensity of the introduced disorder is evaluated by the residual resistivity in the metallic phase under pressure.

A single crystal of κ-Cl used was approximately $0.4 \times 0.4 \times 0.08$ mm^3 in size and thinner than the x-ray attenuation length of 1 mm. The crystal was successively irradiated by white x rays with a nonfiltered tungsten target (40 kV, 20 mA) at room temperature. The dose rate was approximately 0.5 MGy/h [33]. The ^{1}H NMR spectra were obtained by the standard solid-echo method (see also the Supplemental Material [26]). A magnetic field of 3.7 T was applied perpendicular to the conducting ac plane. With this

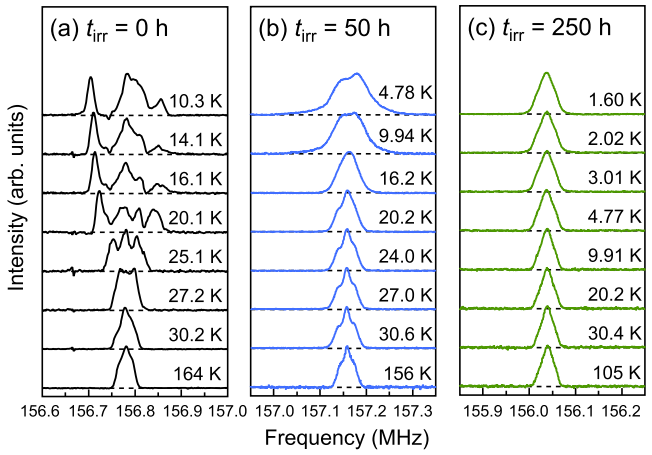

FIG. 1. Temperature dependence of ^{1}H NMR spectra of a successively x-ray-irradiated κ-Cl crystal for t_{irr} = (a) 0 (from Ref. [38]), (b) 50, and (c) 250 h.

field magnitude and configuration, the antiparallel spins in the pristine AF state are oriented parallel to the c axis with slight spin canting in the ab plane [26,37].

Figure 1 shows the temperature dependence of NMR spectra measured after each successive x-ray irradiation. At high temperatures above 30 K, the spectral shape and width remain unchanged as temperature and irradiation time t_{irr} are varied, because the spectral profile is determined by ^{1}H-^{1}H nuclear dipole interactions. The impact of the x-ray irradiation is visible below 30 K. Before irradiation ($t_{irr} = 0$ h), the spectrum splits into discrete lines below 27 K, which evidences a commensurate antiferromagnetic order [38]. After irradiation for 50 h, however, the spectrum shows a structureless broadening below 16 K, indicating the continuous distribution of local moments in magnitude. The structureless profile might suggest an incommensurate order or a spin-glass (SG)-like inhomogeneous frozen state. The observed bell-shaped spectrum, however, rules out the former case, which would give wings at the spectral edges [39,40] (see our spectral simulations in the Supplemental Material [26]). By more irradiation, the spectral broadening is gradually diminished and its onset T_m is lowered: T_m = 12, 8.5, 5.5, 5.0, and 3.9 K for t_{irr} = 70, 90, 120, 150, and 200 h, respectively. Further irradiations for t_{irr} = 250 and 400 h make the line broadening suppressed and its onset not clearly defined.

The spectral width is characterized by the square root of the second moment, $\langle f_{2nd}\rangle^{1/2} = [\int I(f)(f-\langle f\rangle)^2 df / \int I(f) df]^{1/2}$ (with $\langle f\rangle$ the mean frequency), a mean of ^{1}H-site local field magnitudes projected along the direction of the applied field. It increases below T_m and saturates at low temperatures [Fig. 2(a)]. Figure 2(b) shows the irradiation time dependence of the saturation values of $\langle f_{2nd}\rangle^{1/2}$ along with the spectral widths defined by the half-widths at 50% and 2% of the maximum value, $\Delta f_{50\%}$ and $\Delta f_{2\%}$. They all decrease with increasing t_{irr} in similar manners, indicating that the distributed moments tend to shrink on the whole.

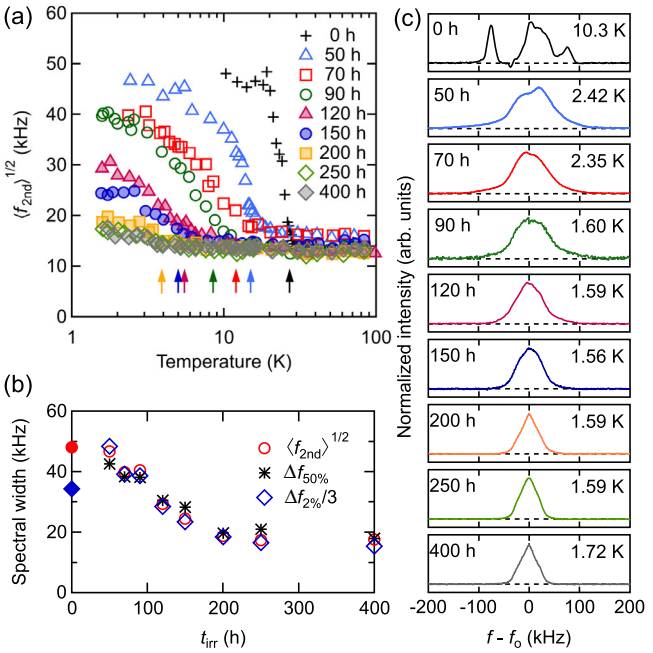

FIG. 2. (a) Temperature dependence of the square root of the second moment $\langle f_{2nd}\rangle^{1/2}$ for different t_{irr}'s. The arrows indicate the onset temperatures at which spectral splitting or broadening starts T_m. (b) Spectral width defined by $\langle f_{2nd}\rangle^{1/2}$, the half widths at 50% and 2% of the maximum value, $\Delta f_{50\%}$ and $\Delta f_{2\%}$, for the spectra at the lowest measured temperature for each t_{irr} shown in (c).

We simulated the spectral shape for inhomogeneous AF orders, assuming the Gaussian-type distribution of local moments (see Supplemental Material [26] for details). However, the spectral shape was not adequately reproduced by the nonuniform AF moments with or without a paramagnetic fraction at least for $t_{irr} \leq 90$ h. Although our simulation is limited to Gaussian distributions, this suggests that the majority of spins take SG-like inhomogeneous configurations below T_m. This is unlike the pristine AF spin structure, whose hallmark is asymmetry in spectrum because antiparallel spins on glide-related ET dimers [Fig. S1(b) in the Supplemental Material [26]] give the same line shifts, when flopped under a field directed in the glide plane, and two degenerate AF orders are unequalized in energy by Dzyaloshinskii-Moriya interaction, thus being single domained [41,42]. The weak asymmetry in the spectra in Fig. 2(c) may signify remaining AF fractions that fade out with irradiation up to t_{irr} = 90 h. For $t_{irr} \geq 120$ h, the spectra are narrowed and symmetrical, likely suggesting a SG-like state with reduced and distributed moments or possibly with a QSL-like fraction. We simulated the spectra assuming AF plus paramagnetic fractions, which however necessitates such broad distribution of reduced AF moments to extinguish the asymmetry (see Supplemental Material [26] for details). We consider it a spurious consequence of the forcible fit with an AF fraction and as representing the SG-like state.

Next, we show the results on the nuclear spin-lattice relaxation. The nuclear magnetization at a time t, $M(t)$, that recovers from its saturation [$M(0) = 0$] was fitted by the stretched exponential $1 - M(t)/M(\infty) = \exp\{-(t/T_1)^{\beta}\}$, with β characterizing the inhomogeneity in the nuclear spin-lattice relaxation rate $1/T_1$, where $M(\infty)$ is the thermal equilibrium value. [We also tried another way of fitting that assumes the Gaussian distribution in $\log_{10}(1/T_1)$ [43,44]; both fittings yielded nearly the same results of $1/T_1$ [26].] The impact of the x-ray irradiation on the relaxation profile is apparent at low temperatures below 5 K [see Fig. 3(a)]. In the initial irradiations of $t_{\rm irr} = 50$ and 70 h, β stays in 0.9–1.0 near the homogeneous limit $\beta = 1$. With more irradiations of $t_{\rm irr} = 90$ and 120 h, β clearly deviates from unity, dropping down to 0.73 at 1.63 K for $t_{\rm irr} = 90$ h; however, further, for $t_{\rm irr} \geq 150$ h, β recovers to above 0.9. These indicate that the relaxation stays rather homogeneous just after the collapse of the AF order but gets inhomogeneous with the disorder increased, most prominently for $t_{\rm irr} = 90$–120 h, and eventually recovers to homogeneous relaxation.

Figure 3(b) shows the temperature dependence of the nuclear spin-lattice relaxation rate $1/T_1$ obtained by the stretched exponential fits for different $t_{\rm irr}$. Below 200 K, the level of $1/T_1$ gradually increases with $t_{\rm irr}$. In general, $1/T_1$ is related to the hyperfine coupling constant $A_{\perp}(\boldsymbol{q})$ and the dynamical spin susceptibility $\chi_{\perp}(\boldsymbol{q}, \omega_o)$, through the form of $1/T_1 \sim k_B T \sum_{\boldsymbol{q}} |A_{\perp}(\boldsymbol{q})|^2 {\rm Im}\chi_{\perp}(\boldsymbol{q}, \omega_o)$, with a wave vector $\boldsymbol{q}$, and the observation frequency ω_o [45]. If $\chi_{\perp}(\boldsymbol{q}, \omega_o)$ is responsible for the increase in $1/T_1$ by irradiation, a conceivable origin is the reduction of magnetic interaction J, to which $1/T_1$ is inversely proportional in paramagnetic insulators. However, the static susceptibility shows no meaningful change or even exhibits decreases, suggesting an increase in J after irradiation [23]. An alternative interpretation is an increase in $A_{\perp}(\boldsymbol{q})$, possibly caused by a conformational change of ethylene groups due to x-ray-induced positional disorder of anions [33,35], because the ^{1}H-site amplitude of the highest occupied molecular orbital, which contributes to $A_{\perp}(\boldsymbol{q})$, can be varied by the ethylene conformation.

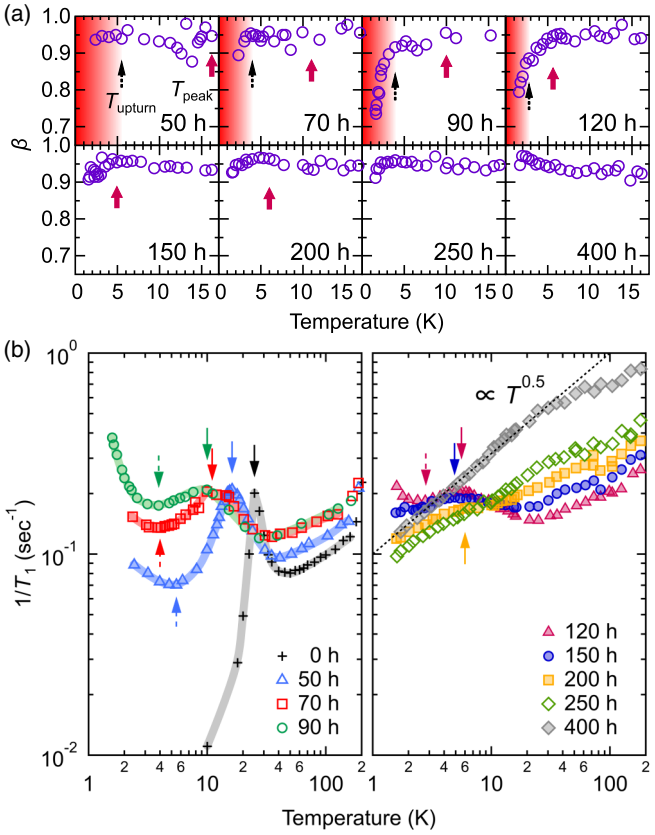

FIG. 3. Temperature dependence of (a) exponent β and (b) ^{1}H nuclear spin-lattice relaxation rate $1/T_1$, obtained by the stretched exponential fits of the relaxation curves. The data for $t_{\rm irr} = 0$ h are from Ref. [38]. The solid and dashed arrows indicate $T_{\rm peak}$ and $T_{\rm upturn}$, respectively.

The temperature profile of $1/T_1$ below 50 K is remarkably changed by x-ray irradiation. Before irradiation, $1/T_1$ forms a sharp peak at the Néel temperature $T_{\rm peak}$ due to slowing down of spin fluctuations and subsequent dropoff of spin wave excitations. By x-ray irradiation, $T_{\rm peak}$ is lowered in parallel with T_m with the peak structure rounded, possibly because of nonuniform spin freezing. The drop in $1/T_1$ below $T_{\rm peak}$ becomes inconspicuous, indicating the enhancement of residual spin fluctuations, and $1/T_1$ gets to show an upturn below several Kelvins most prominently for $t_{\rm irr} = 90$ h [Fig. 3(b)]. The upturn behavior implies residual paramagnetic spins present even below $T_{\rm peak}$, which may freeze at lower temperatures. Such "orphan" spins are predicted theoretically, e.g., as diffusive isolated spins failing to form singlets in the random-bond Heisenberg model on the frustrated two-dimensional lattices [19]. We note that the mostly enhanced upturn of $1/T_1$ emerges from the most inhomogeneous nuclear relaxation at 1.63 K for $t_{\rm irr} = 90$ h [Fig. 3(a)]; the relaxation curve also contains a long T_1 (~100 s) component (with several percent in volume fraction) out of the stretched exponential fit [Fig. S12(k) in Supplemental Material [26]] while the averaged value of $1/T_1$ is 0.4 1/s ($T_1 \sim 2.5$ s). The emergence of such long T_1 components that were absent in the earlier stage of irradiation suggests local singlet formation. Given that a SG-like state and a minor nonuniform AF component are suggested by the NMR spectra, the sample likely consists of highly heterogeneous domains with complicated domain boundaries, which may carry the orphan spins. Similar complex clusterizations are discussed in other frustrated magnets [46,47]. For $t_{\rm irr} \geq 150$ h, the low-temperature upturn and the peak structure of $1/T_1$ are suppressed, leading to the power law of $1/T_1 \sim T^{0.5}$ for $t_{\rm irr} = 400$ h [Fig. 3(b)]—the QSL behavior as previously observed for $t_{\rm irr} = 500$ h [23].

The evolution of the magnetic profile by successive x-ray irradiation is mapped on the plane of the moment-induced

spectral width $\langle f_{2\mathrm{nd}}\rangle_m^{1/2}$ versus spin freezing temperature in Fig. 4. The $\langle f_{2\mathrm{nd}}\rangle_m^{1/2}$, a measure of the averaged moment $\langle m_{\mathrm{loc}}\rangle$, is evaluated by $\sqrt{\langle f_{2\mathrm{nd}}\rangle^{\mathrm{LT}} - \langle f_{2\mathrm{nd}}\rangle^{\mathrm{HT}}}$, where $\langle f_{2\mathrm{nd}}\rangle^{\mathrm{LT}}$ and $\langle f_{2\mathrm{nd}}\rangle^{\mathrm{HT}}$ are the second moments of the spectra below and above T_m, respectively. $\langle f_{2\mathrm{nd}}\rangle^{\mathrm{LT}}$ consists of the moment contribution $\langle f_{2\mathrm{nd}}\rangle_m$ and the temperature-insensitive nuclear dipolar contribution, which is approximated by $\langle f_{2\mathrm{nd}}\rangle^{\mathrm{HT}}$. The irradiations before $t_{\mathrm{irr}} = 100$ h greatly reduce T_m and T_{peak} down to ~5 K with a moderate reduction in $\langle m_{\mathrm{loc}}\rangle$. With further irradiations, however, T_m and T_{peak} cease to decrease and these values become ill-defined, while $\langle m_{\mathrm{loc}}\rangle$ turns to a steep decrease. As such, the randomness-induced route to a QSL from the AF order goes through two different regimes not via the quantum critical point, where T_m and T_{peak} vanish to absolute zero.

Figure 5(a) summarizes the present NMR results of x-ray-irradiated κ-Cl for $t_{\mathrm{irr}} \lesssim 150$ h. The suppression of the pristine AF order is followed by a rapid decrease in the spin freezing temperature T_m or the $1/T_1$ peak temperature T_{peak}, both of which saturate to 5 K. $1/T_1$ exhibits upturns at low temperatures for an intermediate t_{irr} range where spin dynamics is most inhomogeneous, before the system evolves into the gapless QSL state.

Remarkably, the decrease of T_m (or T_{peak}) is more rapid than that of the superconducting transition temperature T_{SC} in the metallic phase under pressure [Figs. 5(b) and 5(c)]. A majority of experiments to date support that the superconductivity in κ-type ET compounds is non-s-wave [31] and disorder sensitive as demonstrated in Refs. [48–50], meaning that the present AF state is much more disorder sensitive than the superconductivity. The fragility of the AF order is also illustrated by referring to the electron mean free path l in the metallic phase, a measure of the mean distance between disorder centers [inset of Fig. 5(a); see also Supplemental Material [26] for details]. Before irradiation, l is several thousand angstroms, indicating that the system is in the clean limit. It is surprising that the collapse of the AF order occurs even under sparse distribution of disorder centers with $l = 200$–700 Å. By further irradiation, l is shortened but stays larger than 100 Å before $t_{\mathrm{irr}} = 100$ h, consistent with the observation of the quantum oscillations in an isostructural ambient-pressure conductor κ-$(\mathrm{ET})_2\mathrm{Cu}(\mathrm{NCS})_2$ with the similar concentration of x-ray-induced disorder centers [49]. When l is reduced from 100 Å, the SG-like state evolves into the QSL-like state with the moments progressively reduced [Figs. 2(b) and 4].

According to the theoretical calculations with the Anderson-Hubbard model [51] and the random-bond Heisenberg model [52] for square lattices, the sublattice moments decrease with increasing disorder, and gapless

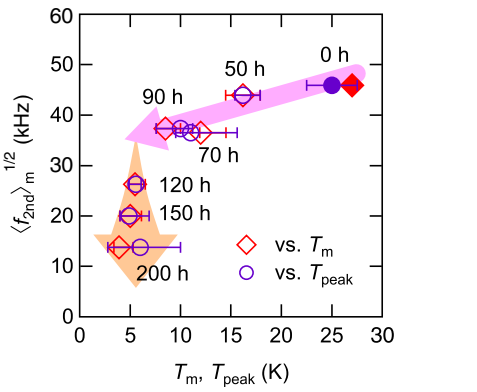

FIG. 4. Square root of the moment contribution to the second moment $\langle f_{2\mathrm{nd}}\rangle_m^{1/2}$ at the lowest measured temperature versus spin freezing temperature, T_m or T_{peak}.

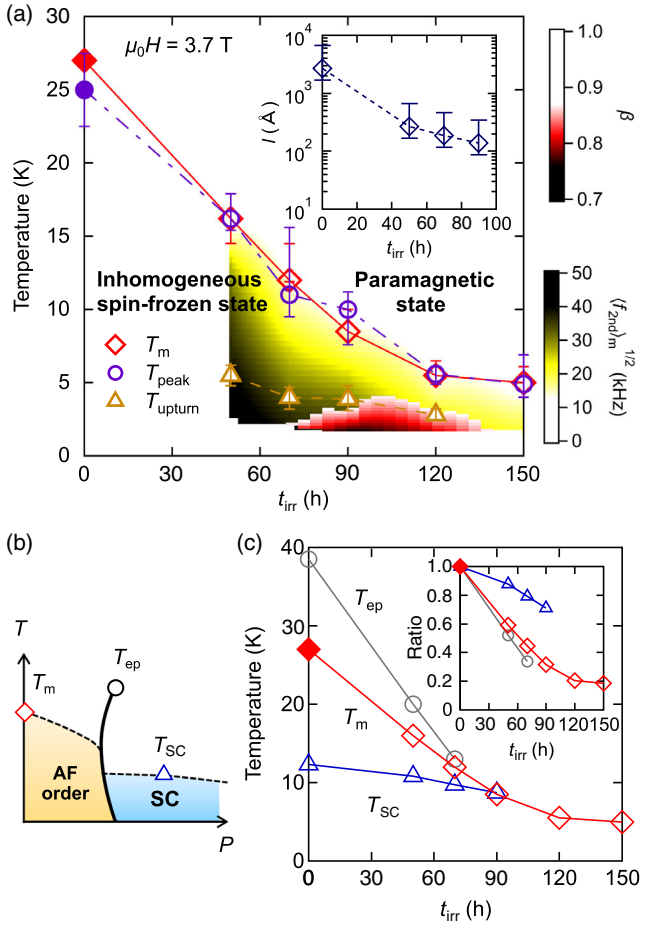

FIG. 5. (a) Temperature-irradiation time phase diagram. The rhombuses and circles indicate the spin freezing temperatures defined by the onset of the spectral broadening T_m and the peak temperature of $1/T_1$, T_{peak}; they nearly coincide. The triangles represent the onsets of upturns in $1/T_1$ on cooling. The magnitudes of β and $\langle f_{2\mathrm{nd}}\rangle_m^{1/2}$ are displayed by a range of colors. (Inset) Irradiation time dependence of the mean free path l deduced from the residual resistivity in the metallic phase under pressure. (b) Schematic pressure-temperature phase diagram. (c) Comparison of T_m (rhombuses), superconducting transition temperature T_{SC} (triangles), and Mott critical end point, T_{ep} (circles); the data of T_{ep} and T_{SC} are taken from Ref. [48]. (Inset) Relative change of T_m, T_{SC}, and T_{ep} from their values before irradiation.

spin states emerge. Similarly, in the case of triangular lattices, the classical 120° spin order is predicted to collapse into a disorder-induced random singlet state of a gapless nature [19,20]. In these models, the suppression of the AF state requires the inhomogeneity of several dozen percent in exchange interactions or transfer integrals, in strong contrast to the present observation that the spin freezing temperature is suppressed by 70% by only a weak randomness that gives $l = 100$–300 Å ($t_{\mathrm{irr}} = 90$ h). This suggests that the disordering of the AF order in κ-Cl is highly nonlocal, possibly pertaining to the vicinity of a Mott transition, where the higher-order and ring exchanges are appreciable and self-conflicting [53]. The emergence of a gapless QSL with a "diffusive spinon metal" [54] or a "spin liquid charge glass" [55] near the Mott-Anderson metal-insulator transition is theoretically proposed. Additionally, the critical end point of the first-order Mott transition in κ-Cl, T_{ep}, drops off similar to T_m with increasing quenched disorder [Fig. 5(c)] and the energy scale of the quantum critical charge fluctuations decreases [48], which can work against spin ordering.

In summary, ^{1}H NMR on the successively x-ray-irradiated Mott insulator κ-Cl clarified how an AF order transitions into a QSL with increasing randomness. The AF order collapses into an inhomogeneous spin frozen state, most likely a SG state, by slight disturbance with disorder centers sparsely distributed at intervals l of hundreds of angstroms and, when further disturbed, grades into a QSL via two regimes. First, the spin freezing temperature T_m decreases (steeper than T_{SC} of the disorder-sensitive nodal superconductivity under pressure) with a moderate reduction in the moments. Next, the moments are diminished with T_m staying around 5 K but getting ill-defined, leading to a QSL with vanishing moments and gapless spin excitations. The first regime for maturing the SG crosses over to the second regime for fostering the QSL around the randomness of $l \sim 100$ Å, where the spin system is so heterogeneous as to include orphan spins and local singlets in the SG-like background. The fragility of an AF order to randomness offers a distinct pathway to a QSL from geometrical frustration.

The authors thank T. Furukawa for experimental supports and discussions. This work was supported by JSPS Grants-in-Aid for Scientific Research (Grants No. JP25220709, No. JP18H05225, No. JP17K05532, and No. JP19H01833) and the Murata Scientific Foundation.

[1] P. W. Anderson, Mater. Res. Bull. **8**, 153 (1973).
[2] P. A. Lee, Science **321**, 1306 (2008).
[3] L. Savary and L. Balents, Rep. Prog. Phys. **80**, 016502 (2017).
[4] Y. Zhou, K. Kanoda, and T.-K. Ng, Rev. Mod. Phys. **89**, 025003 (2017).
[5] Y. Shimizu, K. Miyagawa, K. Kanoda, M. Maesato, and G. Saito, Phys. Rev. Lett. **91**, 107001 (2003).
[6] S. Yamashita, Y. Nakazawa, M. Oguni, Y. Oshima, H. Nojiri, Y. Shimizu, K. Miyagawa, and K. Kanoda, Nat. Phys. **4**, 459 (2008).
[7] M. Yamashita, N. Nakata, Y. Kasahara, T. Sasaki, N. Yoneyama, N. Kobayashi, S. Fujimoto, T. Shibauchi, and Y. Matsuda, Nat. Phys. **5**, 44 (2009).
[8] M. Yamashita, N. Nakata, Y. Senshu, M. Nagata, H. M. Yamamoto, R. Kato, T. Shibauchi, and Y. Matsuda, Science **328**, 1246 (2010).
[9] T. Itou, A. Oyamada, S. Maegawa, and R. Kato, Nat. Phys. **6**, 673 (2010).
[10] S. Yamashita, T. Yamamoto, Y. Nakazawa, M. Tamura, and R. Kato, Nat. Commun. **2**, 275 (2011).
[11] Y. Shen, Y. D. Li, H. Wo, Y. Li, S. Shen, B. Pan, Q. Wang, H. C. Walker, P. Steffens, M. Boehm, Y. Hao, D. L. Quintero-Castro, L. W. Harriger, M. D. Frontzek, L. Hao, S. Meng, Q. Zhang, G. Chen, and J. Zhao, Nature (London) **540**, 559 (2016).
[12] J. A. M. Paddison, M. Daum, Z. Dun, G. Ehlers, Y. Liu, M. B. Stone, H. Zhou, and M. Mourigal, Nat. Phys. **13**, 117 (2017).
[13] J. S. Helton, K. Matan, M. P. Shores, E. A. Nytko, B. M. Bartlett, Y. Yoshida, Y. Takano, A. Suslov, Y. Qiu, J.-H. Chung, D. G. Nocera, and Y. S. Lee, Phys. Rev. Lett. **98**, 107204 (2007).
[14] A. Olariu, P. Mendels, F. Bert, F. Duc, J. C. Trombe, M. A. de Vries, and A. Harrison, Phys. Rev. Lett. **100**, 087202 (2008).
[15] T. Han, S. Chu, and Y. S. Lee, Phys. Rev. Lett. **108**, 157202 (2012).
[16] M. A. de Vries, J. R. Stewart, P. P. Deen, J. O. Piatek, G. N. Nilsen, H. M. Ronnow, and A. Harrison, Phys. Rev. Lett. **103**, 237201 (2009).
[17] Y. Okamoto, M. Nohara, H. Aruga-Katori, and H. Takagi, Phys. Rev. Lett. **99**, 137207 (2007).
[18] Y. Singh, Y. Tokiwa, J. Dong, and P. Gegenwart, Phys. Rev. B **88**, 220413(R) (2013).
[19] H. Kawamura and K. Uematsu, J. Phys. Condens. Matter **31**, 504003 (2019).
[20] K. Watanabe, H. Kawamura, H. Nakano, and T. Sakai, J. Phys. Soc. Jpn. **83**, 034714 (2014).
[21] T. Shimokawa, K. Watanabe, and H. Kawamura, Phys. Rev. B **92**, 134407 (2015).
[22] J.-J. Wen, S. M. Koohpayeh, K. A. Ross, B. A. Trump, T. M. McQueen, K. Kimura, S. Nakatsuji, Y. Qiu, D. M. Pajerowski, J. R. D. Copley, and C. L. Broholm, Phys. Rev. Lett. **118**, 107206 (2017).
[23] T. Furukawa, K. Miyagawa, T. Itou, M. Ito, H. Taniguchi, M. Saito, S. Iguchi, T. Sasaki, and K. Kanoda, Phys. Rev. Lett. **115**, 077001 (2015).
[24] H. C. Kandpal, I. Opahle, Y.-Z. Zhang, H. O. Jeschke, and R. Valentí, Phys. Rev. Lett. **103**, 067004 (2009).
[25] T. Koretsune and C. Hotta, Phys. Rev. B **89**, 045102 (2014).
[26] See Supplemental Material at http://link.aps.org/supplemental/10.1103/PhysRevLett.124.117204 for the supporting results and discussion, which includes Refs. [27–29].
[27] S. M. De Soto, C. P. Slichter, A. M. Kini, H. H. Wang, U. Geiser, and J. M. Williams, Phys. Rev. B **52**, 10364 (1995).
[28] K. Miyagawa, A. Kawamoto, and K. Kanoda, Phys. Rev. Lett. **89**, 017003 (2002).

[29] K. Momma and F. Izumi, J. Appl. Crystallogr. **44**, 1272 (2011).
[30] M. Ito, T. Uehara, H. Taniguchi, K. Satoh, Y. Ishii, and I. Watanabe, J. Phys. Soc. Jpn. **84**, 053703 (2015).
[31] K. Miyagawa, K. Kanoda, and A. Kawamoto, Chem. Rev. **104**, 5635 (2004).
[32] K. Kanoda and R. Kato, Annu. Rev. Condens. Matter Phys. **2**, 167 (2011).
[33] T. Sasaki, Crystals **2**, 374 (2015).
[34] N. Yoneyama, K. Furukawa, T. Nakamura, T. Sasaki, and N. Kobayashi, J. Phys. Soc. Jpn. **79**, 063706 (2010).
[35] N. Yoneyama, T. Sasaki, N. Kobayashi, K. Furukawa, and T. Nakamura, Physica (Amsterdam) **405B**, S244 (2010).
[36] L. Kang, K. Akagi, K. Hayashi, and T. Sasaki, Phys. Rev. B **95**, 214106 (2017).
[37] R. Ishikawa, H. Tsunakawa, K. Oinuma, S. Michimura, H. Taniguchi, K. Satoh, Y. Ishii, and H. Okamoto, J. Phys. Soc. Jpn. **87**, 064701 (2018).
[38] K. Miyagawa, A. Kawamoto, Y. Nakazawa, and K. Kanoda, Phys. Rev. Lett. **75**, 1174 (1995).
[39] R. Blinc, Phys. Rep. **79**, 331 (1981).
[40] T. Takahashi, Y. Maniwa, H. Kawamura, and G. Saito, J. Phys. Soc. Jpn. **55**, 1364 (1986).
[41] D. F. Smith, S. M. De Soto, C. P. Slichter, J. A. Schlueter, A. M. Kini, and R. G. Daugherty, Phys. Rev. B **68**, 024512 (2003).
[42] F. Kagawa, Y. Kurosaki, K. Miyagawa, and K. Kanoda, Phys. Rev. B **78**, 184402 (2008).
[43] V. F. Mitrović, M.-H. Julien, C. de Vaulx, M. Horvatić, C. Berthier, T. Suzuki, and K. Yamada, Phys. Rev. B **78**, 014504 (2008).
[44] A. P. Dioguardi, M. M. Lawson, B. T. Bush, J. Crocker, K. R. Shirer, D. M. Nisson, T. Kissikov, S. Ran, S. L. Bud'ko, P. C. Canfield, S. Yuan, P. L. Kuhns, A. P. Reyes, H.-J. Grafe, and N. J. Curro, Phys. Rev. B **92**, 165116 (2015).
[45] T. Moriya, J. Phys. Soc. Jpn. **18**, 516 (1963).
[46] M.-H. Julien, V. Simonet, B. Canals, R. Ballou, A. K. Hassan, M. Affronte, V. O. Garlea, C. Darie, and P. Bordet, Phys. Rev. B **87**, 214423 (2013).
[47] A. Zorko, O. Adamopoulos, M. Komelj, D. Arčon, and A. Lappas, Nat. Commun. **5**, 3222 (2014).
[48] M. Urai, T. Furukawa, Y. Seki, K. Miyagawa, T. Sasaki, H. Taniguchi, and K. Kanoda, Phys. Rev. B **99**, 245139 (2019).
[49] T. Sasaki, H. Oizumi, Y. Honda, N. Yoneyama, and N. Kobayashi, J. Phys. Soc. Jpn. **80**, 104703 (2011).
[50] J. G. Analytis, A. Ardavan, S. J. Blundell, R. L. Owen, E. F. Garman, C. Jeynes, and B. J. Powell, Phys. Rev. Lett. **96**, 177002 (2006).
[51] M. Ulmke and R. T. Scalettar, Phys. Rev. B **55**, 4149 (1997).
[52] A. W. Sandvik and M. Vekic, Phys. Rev. Lett. **74**, 1226 (1995).
[53] O. I. Motrunich, Phys. Rev. B **72**, 045105 (2005).
[54] A. C. Potter, M. Barkeshli, J. McGreevy, and T. Senthil, Phys. Rev. Lett. **109**, 077205 (2012).
[55] K.-S. Kim, Phys. Rev. B **73**, 235115 (2006).